Article:
Jia, J, Babatunde, A and Wang, M (2015) Void Fraction Measurement of Gas-Liquid Two-Phase Flow from Differential Pressure. Flow Measurement and Instrumentation, 41. 75 - 80. ISSN 0955-5986

https://doi.org/10.1016/j.flowmeasinst.2014.10.010

Void Fraction Measurement of Gas-Liquid Two-Phase Flow from Differential Pressure

Jiabin Jia[b], Akintayo Babatunde[a] and Mi Wang[a*]

[a]School of Chemical and Process Engineering, University of Leeds, LS2 9JT, UK
[b]School of Engineering, University of Edinburgh, Edinburgh, EH9 3JL , UK
jiabin.jia@ed.ac.uk, rinade@msn.com, m.wang@leeds.ac.uk

Abstract: Void fraction is an important process variable for the volume and mass computation required for transportation of gas-liquid mixture in pipelines, storage in tanks, metering and custody transfer. Inaccurate measurement would introduce errors in product measurement with potentials for loss of revenue. Accurate measurement is often constrained by invasive and expensive online measurement techniques. This work focuses on the use of cost effective and non-invasive pressure sensors to calculate the gas void fraction of gas-liquid flow. The differential pressure readings from the vertical upward bubbly and slug air-water flow are substituted into classical mathematical models based on energy conservation to derive the void fraction. Electrical Resistance Tomography (ERT) and Wire-mesh Sensor (WMS) are used as benchmark to validate the void fraction obtained from the differential pressure. Consequently the model is able to produce reasonable agreement with ERT and WMS on the void fraction measurement. The effect of the wall friction on the mathematical models is also investigated and discussed. It is concluded the friction loss cannot be neglected, particularly when gas void fraction is less than 0.2.
Keywords: Differential pressure, void fraction, frictional pressure loss

1. INTRODUCTION

Two-phase flow is any type of flow containing more than one phase of liquid, gas or solid. These processes are frequently encountered in the process industries. Mean volumetric void fraction is a key parameter to characterise two-phase flows. Many researches were carried out to correlate differential pressure and void fraction in two-phase flow, but hindered by inability to generate one model that was valid for all flow regimes. This is due to the complex nature of the different flow patterns and energy interactions in flow [1]. Lockhart and Martinelli [2] gave the general correlation of pressure drop for two-phase flow. Wallis [3] fitted an equation to the plot of liquid hold up *"1-*α_g*"* against Lockhart and Martinelli *"X"* parameter which was a function of the two-phase pressure drop. This postulate implies that the pressure drop in the two-phase flow is higher than that of gas phase or liquid phase alone, because the gas phase is involved in irreversible work on the liquid phase and the presence of more than one phase in the flow conduit reduces available cross sectional area of flow for either fluids present in the two-phase flow. In support of the Lockhart and Martinelli correlation, Merchuk and Stein [4] came up with another correlation by including the impact of all the energies acting on the multiphase flow mechanism quantified as pressure drop due to frictional force. Tang and Heindel [5] further stated that pressure drop of two-phase flow was partially because of mechanisms within the system which caused energy losses, namely; the frictional force existing between flowing fluid and conduit internal surface. It also came from turbulence between the liquid and the gas phases, due to the slip ratio, which was the difference in velocities of two phases. On the contrary the frictional pressure drop was neglected by Hasan [6] and Shafquet et al. [7] on ground that it was negligible because the mass flow rate of the liquid phase was far higher than that of the gas phase. A comparison of results from different authors on multiphase pressure drop was done by Müller-Steinhagen and Heck [8] to match many correlations for two-phase pressure drop. This analysis showed a large variation over the different correlations given by different authors applying to the same experiment. Gharat and Joshi [9] also made a similar analysis by comparing results from another 15 authors some already in by Müller-Steinhagen and Heck's analysis [8] and attributed the discrepancies to inability of the models to be valid across various flow regimes. According to Gharat and Joshi [9], the two-phase frictional pressure loss was dependent on two mechanisms, first was shear stress due to turbulence on the conduit wall and secondly due to presence of bubbles in the mixture, with some additional parameters like eddy diffusivity of bubble and mixing length.

Electrical Resistance Tomography (ERT) and Wire-mesh Sensor (WMS) are tomographic modalities and they have more complicated measurement mechanism than pressure sensors. Both ERT and WMS can measure gas void fraction without the consideration of friction loss in the two-phase flow, which provides an alternative approach to validate the gas void fraction model based on differential pressure. The void fraction measurement accuracy of ERT and WMS were discussed by Faraj [10] and Sharaf [11]. The principle behind ERT is to determine the electrical conductivity by measuring the voltage between the ERT electrodes mounted on the internal circumference of the conveying conduit. The measured conductivity is subjected to the Maxwell's equation [12] to calculate the local cross-sectional void fraction of the dispersed phase. This is an invasive but non-intrusive local void fraction measurement technique in two-phase mixtures, which is also capable of providing tomographic cross-sectional images. WMS consists of two planes of wire electrodes arranged perpendicularly to each other at an angle of 90 degrees covering the flowing cross-sectional area. One plane of the wires is the current transmitter while the other plane is the current receiver. The conductivity is measured by injecting a voltage pulse into one of the transmitting wires, while the other transmitting wires are kept at ground voltage [13], the current flowing to all receiving wires are measured simultaneously and conductivity estimate made from that. The void fraction of gas is derived from the normalised conductivity. Both ERT and WMS can present local cross-sectional void fraction. All local void fractions are averaged to obtain the mean void fraction.

2. EXPERIMENT SETUP AND PROCEDURES

The experiment was carried out on the flow loop facility at the University of Leeds. The sketch of the flow loop is shown in Figure 1. In the experiment, air and tap water are gas and liquid phase respectively. The channel in blue represents the water flow and the red channel represents the air supply. The cyan section represents the mixed air-water flow. The stabilised air flow rate is regulated by the air mass flow controller. After the loop bend, the upwards air-water mixture goes through the flow instrumentations, 5.80 m horizontal section and then back to the water tank, where air is released and water is recycled. The detailed information on flow meters was described in literature [12].

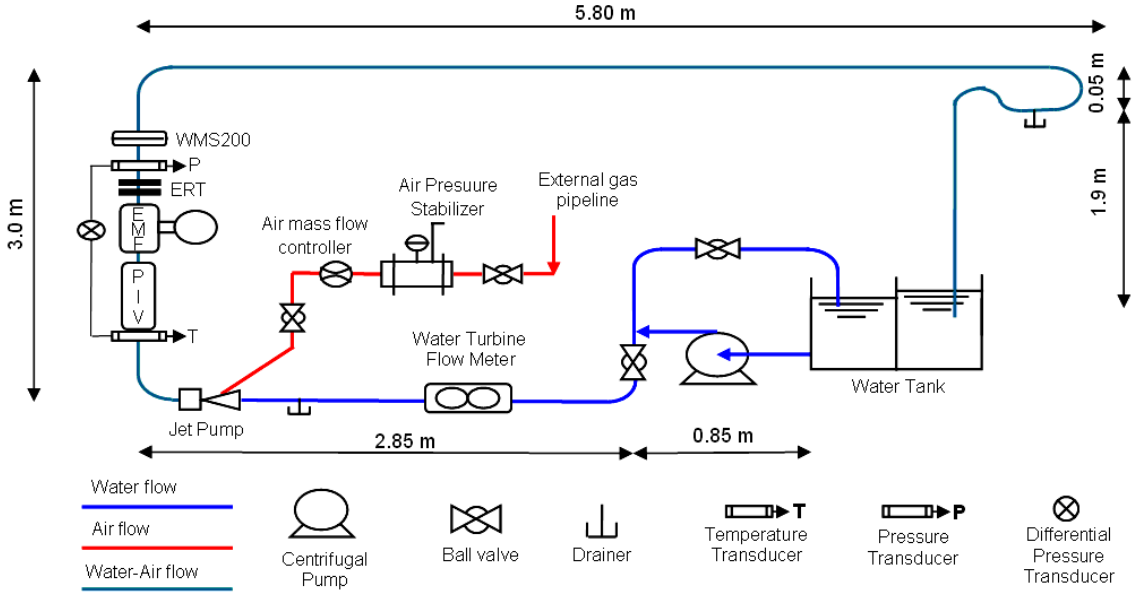

Figure 1. Experimental flow loop

This flow loop only can create bubble and slug two flow regimes. As indicated in Table 1, bubble flow regime was created from the cross combination between three inlet water flow rates and five inlet air flow rates. Slug flow regime was created from the cross combination between three inlet water flow rates and eight inlet air flow rates.

Table 1. Inlet flow rates of air and water

Bubble flow		Slug flow	
Water flow rate (m^3/s)	Air flow rate (m^3/s)	Water flow rate (m^3/s)	Air flow rate (m^3/s)
2.04×10^{-3}	8.33×10^{-5}	9.32×10^{-4}	5.00×10^{-4}
1.45×10^{-3}	1.67×10^{-4}	6.72×10^{-4}	5.83×10^{-4}
8.02×10^{-4}	2.50×10^{-4}	4.11×10^{-4}	6.67×10^{-4}
	3.33×10^{-4}		7.50×10^{-4}
	4.17×10^{-4}		8.33×10^{-4}
			9.17×10^{-4}
			1.00×10^{-3}
			1.08×10^{-3}

A wet/wet differential pressure sensor with two tubes was adopted first. It was not suitable for the air-water flow measurement, because the small air bubbles entering the tube affected the accuracy of readings. The diaphragm gauge pressure sensor was tested later. It worked well when the pressure inside the loop was larger than that of atmosphere, however, because of the working principle of the gauge pressure sensor, it failed to provide the correct readings if the pressure inside the loop was less than atmospheric pressure. Eventually two absolute pressure sensors (Omega PXM209) with 0~2.50 bar measurement range and 0.25% full scale accuracy were selected. The differential pressure is obtained from the subtraction of two individual absolute pressure sensors. The front-end interface of the pressure sensor is intrusive but non-invasive with fluids. The schematic of the experimental sensors is shown in Figure 2 below. Wire-mesh sensor, ERT sensor and electromagnetic flowmeter (EMF) are installed along the vertical Perspex pipe with 500 mm inner diameter. Two absolute pressure sensors are 600mm apart.

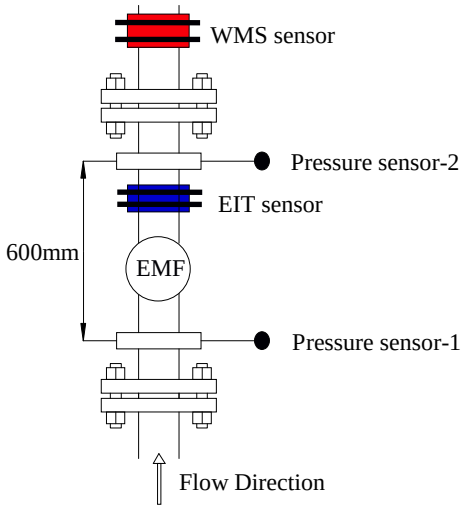

Figure 2. Installation of flow meters

Before dynamic experiment, the pressure sensors were calibrated against atmospheric pressure and static water head to eliminate the systemic error. After each water flow had been established steadily in the flow loop, reference measurement concurrently was taken for ERT and WMS. The pressure readings were sampled via a data acquisition system with 16 bits resolution of analogue to digital conversion. Upon completion of measurement taken for reference, the flow rate of water was kept constant while air was introduced at different flow rates controlled via the gas mass flow rate controller. Once the air flow rate was stable, ERT, WMS and pressure readings were taken concurrently for 10 seconds to get the mean value. The experiment procedures were repeated for different flow conditions.

While the above process was running, readings were also taken for water flow rate via the turbine flow meter, air flow rate via the mass flow meter and water velocity via the electromagnetic flow meter (EMF). The fluid temperature was monitored throughout the whole process. Once all the data had been downloaded, numerical correlations shown in the next section were conducted on the data to estimate the air volumetric void fraction.

3. DIFFERENTIAL PRESSURE CORRELATION FOR VOID FRACTION

The correlation of differential pressure and void fraction is based on the classical Bernoulli's principle of energy conservation within a flowing conduit, which states that as shown in equation (1), the sum of all forms of mechanical energy in a steady fluid along a pipeline is the same at all points.

$$\frac{1}{2}\rho v^2 + \rho gh + P = \text{constant} \tag{1}$$

where $\frac{1}{2}\rho v^2$ is kinetic energy, ρgh is potential energy and P is pressure.

If considering the two tapping points where the pressure sensors are located, equation (1) can be developed as equation (2).

$$\frac{1}{2}\rho_m v_1^2 + \rho_m g h_1 + P_1 = \frac{1}{2}\rho_m v_2^2 + \rho_m g h_2 + P_2 + F_p \tag{2}$$

where ρ_m is gas-liquid mixture density, F_p is frictional pressure loss. Since the pipe is of uniform cross-sectional area. It is assumed force due to velocity of fluid is constant, $v_1 = v_2 = v$, therefore, the kinetic energy on both sides are cancelled.

$$\rho_m g h_1 + P_1 = \rho_m g h_2 + P_2 + F_p \tag{3}$$

The tapping point of the pressure sensor 1 is regarded as reference point with the height $h_1 = 0$ and the height of pressure sensor 2 is $h_2 = h$. Equation (3) above is simplified to

$$P_1 = \rho_m g h + P_2 + F_p \tag{4}$$

Therefore differential pressure ΔP between tapping point 1 and 2 is

$$\Delta P = P_1 - P_2 = \rho_m g h + F_p \tag{5}$$

In gas-liquid two-phase flow, the mixture density ρ_m is defined from gas density ρ_g and liquid density ρ_l.

$$\rho_m = (1 - \alpha_g)\rho_l + \alpha_g \rho_g \tag{6}$$

Substituting equation (6) into equation (5) gives

$$\Delta P = [(1 - \alpha_g)\rho_l + \alpha_g \rho_g] g h + F_p \tag{7}$$

Solving for void fraction α_g from the equation (7) gives

$$\alpha_g = \frac{\Delta P - \rho_l g h - F_p}{(\rho_g - \rho_l) g h} \tag{8}$$

The frictional pressure loss F_p is defined as

$$F_p = \frac{2C_f \rho_m h v^2}{D} \tag{9}$$

Before F_p is computed, the actual liquid velocity v and the Fanning friction factor C_f have to be predetermined. C_f is formulated into different format in terms of the different flow conditions and the roughness of the pipe wall. The material of the pipe is Perspex, which has relatively smooth wall. In out experiment, the Reynolds numbers ($Re=\rho vD/\mu$) of all flow conditions are in the range of 3,000~100,000, therefor Fanning friction factor C_f is simplified as the form in equation (10).

$$C_f = 0.079\,Re^{-0.25} \tag{10}$$

For simplicity, water dynamic viscosity μ is taken in Reynolds number. Air density ρ_g is approximated to 0 because it is nearly 1000 times less than water density ρ_l and the mass flow rate of water much is larger than the mass flow rate of air, which caused 0.12% error of void fraction by this approximation.

Due to the complex nature of the gas-liquid two-phase flow, the on-line acquisition of the actual liquid velocity v and viscosity μ remain a challenge, which hampers the accuracy of Fanning friction factor C_f obtained. In our study, the liquid velocity v is approximated from the division of the commingled flow rate reading on the electromagnetic flow meter (EMF) and the internal cross-sectional area of the EMF port. This velocity is an indication of the actual liquid velocity and not the superficial velocity based on the principle of operation of the EMF meter. Fluids temperature is monitored to calibrate water viscosity and density for calculating the Reynolds number. Applying these assumptions and substituting equation (9) into equation (8), void fraction α_g is expressed as

$$\alpha_g = 1 - \frac{\Delta P}{\rho_l g h} + \frac{2C_f v^2}{gD} \tag{11}$$

4. RESULTS AND DISCUSSION

4.1. Void Fraction from Differential Pressure

Figure 3 indicates the relationship between air/water flow rate and differential pressure. The different colour symbols represent different inlet water flow rate. When inlet water flow rate is kept constant, differential pressure decreases with the increase of inlet air flow rate. When inlet air flow rate remains constant, differential pressure decreases with the decrease of inlet water flow rate.

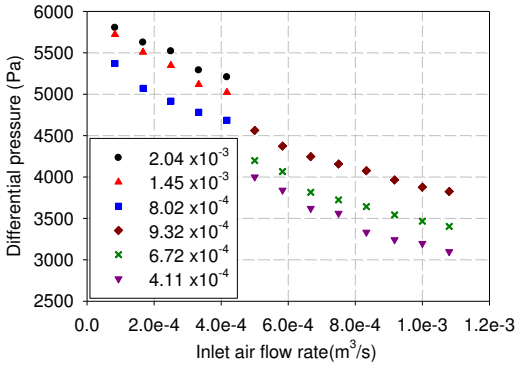

Figure 3. Variation of differential pressure with air/water flow rate
(Inlet water flow rates are presented with different legend)

Differential pressure subtracted from two absolute pressure sensors was fed into mathematical model in equation (11). The change of air void fraction with air/water flow rate is illustrated in Figure 4. Void fraction increases with the increase of inlet air flow rate, when inlet water flow rate is constant. Void fraction increases with the decreases of inlet water flow rate, when inlet air flow rate is constant.

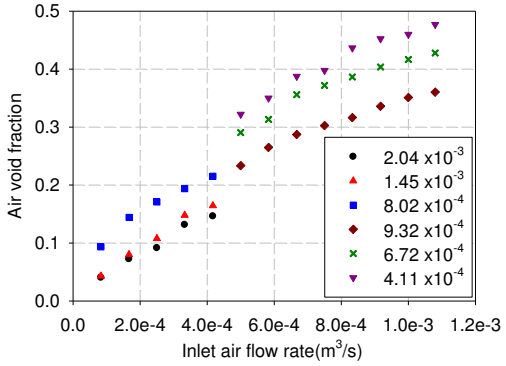

Figure 4. Variation of air void fraction with air/water flow rate

4.2. Comparison with ERT and WMS

To ensure the precision of the ERT and WMS air void fraction measurement on air-water flow, four flow conditions were configured. The experiment was repeated five times. The mean air void fraction and corresponding standard deviation of each flow condition is listed in Table 2. Data in Table 2 is exhibited in Figure 5 to show the standard deviation in the form of error bar. It is shown that the precision of ERT and WMS is on the same scale and it is difficult to conclude the superiority of two tomographic modalities. However it is noticed that ERT has smaller measurement variation than WMS when air void fraction is less than 0.05.

Table 2. Precision of ERT and WMS air void fraction measurement

Water flow rate (m^3/s)	Air flow rate (m^3/s)	Mean air void fraction from ERT	Standard deviation	Mean air void fraction from WMS	Standard deviation
2.04×10^{-3}	8.33×10^{-5}	3.948×10^{-2}	1.066×10^{-3}	4.145×10^{-2}	5.951×10^{-3}
2.04×10^{-3}	8.33×10^{-4}	2.105×10^{12}	9.312×10^{-3}	2.266×10^{-1}	3.504×10^{-3}
9.32×10^{-4}	8.33×10^{-5}	7.2535×10^{-2}	8.303×10^{-3}	6.724×10^{-2}	8.608×10^{-3}
9.32×10^{-4}	8.33×10^{-5}	2.9707×10^{-1}	3.148×10^{-3}	3.043×10^{-1}	7.017×10^{-3}

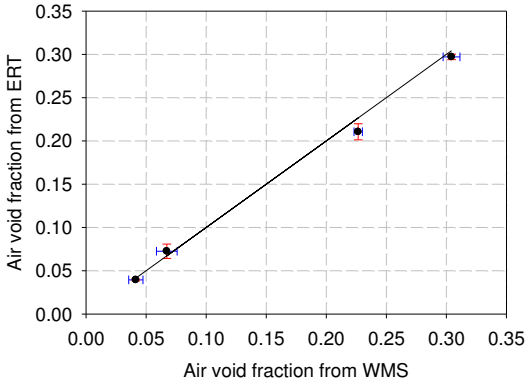

Figure 5. Precision of ERT and WMS air void fraction measurement

All the void fractions obtained at different combinations of air and water flow rate in Table 1 are plotted in Figure 5, where differential pressure (DP) model agrees with the guiding principles that void fraction increases with

gas superficial velocity and vice versa. This is because, in the bubble flow regime, the void fraction is less due to the large volume of water that comingles with the air in this regime, this causes more drag on the dispersed gas bubbles preventing them to move through the continuous liquid phase thereby reducing the void fraction, but a change in trend is seen in the slug flow regime when the gas superficial velocity is increased given the air bubbles more energy in moving up through the continuous water phase without the drag noticed in the bubble flow regime.

Comparison between ERT and WMS has been discussed in pervious literature [12]. ERT and WMS have good agreement when air void fraction is less than 0.25. However, it is apparently noticed that the void fraction from ERT is underestimated when void fraction is more than 0.25. Void fraction from DP model has great match with WMS void fraction estimations, particularly if void fraction is larger than 0.2. It is also noticed that void fraction from DP model has larger discrepancy with that from WMS when air void fraction is less than 0.2. The reason might because at these flow conditions, the absolute pressure readings belong to the lower range of pressure sensor's full measurement range, although differential pressure between two pressure sensors is larger (5000~6000 Pa in Figure 3). A standard differential pressure sensor should overcome this problem. The term of frictional pressure loss in equation (8) plays an important role towards calculating void fraction less than 0.2. Section 4.3 focuses on the discussion on this issue.

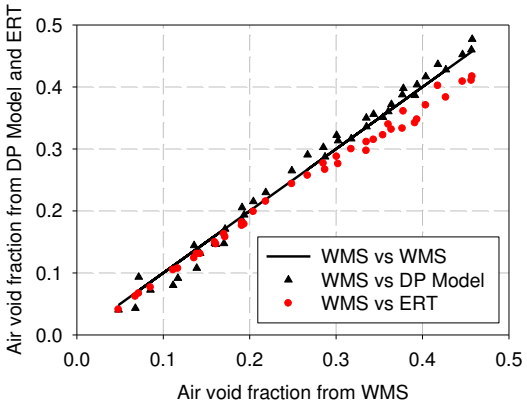

Figure 6. Air void fraction comparison for WMS, ERT and DP Model

4.3. Impact of Frictional Pressure Loss on Void Fraction Estimation

The impact of neglecting the frictional pressure loss is further analysed on DP model. Figure 7 illustrates the relative difference of air void fraction when frictional pressure loss is included or neglected. The solid curve in Figure 7 represents the trend line of the points. Figure 7 shows that the impact of friction on the air void fraction. Generally, the smaller the air void fraction is the greater relative difference with and without taking pipe wall friction into equation (8). When air void fraction is larger than 0.2, the relative difference is less than 3% and the frictional pressure loss is somewhat negligible. However when air void fraction is 0.15, the relative difference reaches 10% and keeps increasing to 65% at void fraction 0.04 which means pipe wall friction has more significant effects.

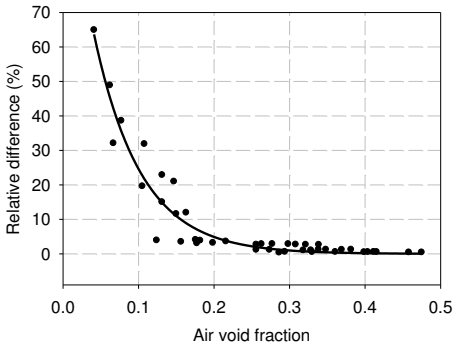

Figure 7. Relative difference with and without pipe wall friction

5. CONCLUSIONS

Two absolute pressure sensors are used to measure differential pressure. The method has benefits of low capital cost and ease of installation, however, the accuracy of pressure measurement might not be sufficient at the lower range of sensor's full scale. The differential pressure model based on energy conservation is re-derived based on a few assumptions. Experimental results show that the void fractions obtained from differential pressure model has good agreement with those obtained from Electrical Resistance Tomography and Wire-mesh sensor. Results also show that the term of pipe wall friction in differential pressure model has larger effect on the air-water flow with smaller air void fraction. This term cannot be neglected when air void fraction is smaller than 0.2. When air void fraction is larger than 0.2, the relative difference of void fraction caused by neglecting pipe wall friction is less than 3%. In summary these findings will help in the estimation of void fraction for multiphase flow systems, which will serve as a platform for further engineering studies in the area of multiphase flow metering.

REFERENCES

1. Á. G. Német, "Maximum Liquid Transport. Flow of Gas-Liquid Mixtures in Vertical Tubes", Industrial & Engineering Chemistry, 53, 1961, pp. 151-154.
2. R. W. Lockhart and R. C. Martinelli, "Proposed Correlation of Data for Isothermal Two-Phase, Two component Flow in Pipes". Chemical Engineering Process, 45, 1949, pp. 39-49.
3. G. B. Wallis, One Dimensional Two Phase Flow, USA, McGraw-Hill Book Company, 1969.
4. J. C. Merchuk and Y. Stein, "Local Hold-up and Liquid Velocity in Air-lift Reactors". AIChE Journal, 27, 1981, pp. 377-388.
5. C. Tang and T. J. Heindel, "Estimating Gas Holdup via Pressure Difference Measurements in a Cocurrent Bubble Column". International Journal of Multiphase Flow, 32, 2006, pp. 850-863.
6. A. H. Hasan, "Multiphase Flow Rate Measurement Using a Novel Conductance Venturi Meter: Experimental and Theoretical Studi in Different Flow Regimes". Ph.D. Thesis, University of Huddersfield, 2010.
7. A. Sharquet, I. Ismail and M. N. Karsiti, "Study of Void Fraction Measurement in a Two Phase Flow by Using Differential Pressure and Electrical Capacitance Tomography". Mathematical/Analytical Modelling and Computer Simulation (AMS), Fourth Asia International Conference on, 26-28 May 2010, pp. 408-413.
8. H. Müller-Steinhagen and K. Heck, "A Simple Friction Pressure Drop Correlation for Two-phase Flow in Pipes". Chemical Engineering and Processing: Process Intensification, 20, 1986, pp.297-308.
9. S. D. Gharat and J. B. Joshi, "Transport Phenomena in Bubble Colunm Reactor II: Pressure Drop", The Chemical Engineering Journal, 48, 1992, pp. 153-166.
10. Y. Faraj, M. Wang, J. Jia, Q. Wang, C. Xie, G. Oddie, K. Primrose and C. Qiu, "Measurement of Vertical Oil-in-water Two-phase Flow Using Dual modality ERT EMF System", 5th International Workshop on Process Tomography, Jeju, Korea, September 16-18, 2014.
11. S. Sharaf, M. Da Silva, U. Hampel, C. Zippe, M. Beyer and B. Azzopardi, "Comparison between wire mesh sensor and gamma densitometry void measurements in two-phase flows", Measurement Science and Technology Vol. 22, Issue 10, 2011.
12. C. Olerni, J. Jia and M. Wang, "Measurement of Air Distribution and Void Fraction of an Upward Air-water Flow Using Electrical Resistance Tomography and Wire-mesh Sensor", Measurement Science and Technology Vol. 24, Issue 3, 2013.
13. H. -M. Prasser, M. Misawa and I. Tiseanu, "Comparison between Wire-mesh Sensor and Ultra-fast X-ray Tomograph for an Air-water Flow in a Vertical Pipe". Flow Measurement and Instrumentation, 16, 2005, pp. 73-83.

Nomenclature

- ρ *is* density
- v is velocity
- g is acceleration due to gravity
- h is static head above pressure tapping point
- P is pressure
- F_p is frictional pressure loss
- α *is the gas void fraction*
- ΔP *is differential pressure*
- C_f is fanning friction factor
- D is internal diameter of pipe
- Re is Reynolds number
- μ is viscosity

Subscripts

- m is mixture
- g is gas
- l is liquid
- p is pipe
- 1 & 2 are sensor positions